Int. J. Multiphase Flow Vol. 12, No. 5, pp. 711–732, 1986
Printed in Great Britain.

0301-9322/86 $3.00 + 0.00

MODELLING OF ANNULAR DISPERSED TWO-PHASE FLOW IN VERTICAL PIPES

R. V. A. OLIEMANS, B. F. M. POTS and N. TROMPÉ
Koninklijke/Shell-Laboratorium, Shell Research B. V., Amsterdam, The Netherlands

(*Received* 15 *April* 1985; *in revised form* 4 *November* 1985)

Abstract—An investigation is made into the reliability with which pressure loss, film thickness and liquid entrainment can be predicted by an annular flow model that is based on the well-known two-fluid (separated flow) concept. For this purpose a two-fluid model is presented which accounts for the interrelation between these variables. In this connection the existence of multiple liquid hold-up solutions is mentioned. New correlations for interfacial friction and liquid fraction entrained are proposed using data compiled previously at AERE Harwell. Our new model is compared with previous models. Differences between predictions are illustrated by reference to the Harwell data bank, recent large-diameter tests and hypothetical gas-well cases relevant to the oil industry. Application of the annular flow models, in particular their entrainment correlations, appears to give rise to widely varying results, restricting the predictive value of the models when extrapolated to large-diameter and/or high pressure systems.

1. INTRODUCTION

Annular dispersed flow is a two-phase flow regime, which in the oil industry is of importance in, for example, the production as well as transportation of gas/condensate and gas/oil systems. It is predicted to exist in risers connected to horizontal flow lines and in vertical tubing of gas wells (with simultaneous production of condensate and water). In this flow regime the gas stream—with a certain amount of liquid entrained as droplets—flows in the pipe centre, while the remainder of the liquid flows as a thin film in contact with the pipe wall. For a proper design of downstream facilities it is important to know the amount of liquid that travels with the gas stream in the form of droplets. Information on the liquid-film characteristics (thickness, residence time of liquid) is of relevance for erosion and corrosion aspects. Accurate pressure-drop predictions are required in hydraulic piping designs.

The conditions of the fluids in the above applications (gas/condensate or gas/oil systems at, typically, a pressure of 20 MPa) generally differ widely from those in experimental systems for which vertical annular tests have been carried out. In the Harwell data bank for vertical annular flow (Whalley & Hewitt 1978), for instance, the conditions of the atmospheric air/water measurements are markedly different, while the physical properties for the 7 MPa steam/water system have values that are intermediate between those for an atmospheric air/water system and a 20 MPa gas/condensate system. An additional concern in scaling is the difference in pipe size: gas-well tubing is sized at 100–150 mm, whereas the vertical flow data relate to pipes with sizes of 20–30 mm. Furthermore, most laboratory data have been obtained in relatively short pipes, so that one cannot rule out possible entrance effects on the measured data, while for tubing lengths of 600–3000 m one requires data that are completely free of such effects.

In the oil industry, two-phase flow calculation methods for vertical upflow are mainly empirical and have a limited validity range. Well-known schemes like those of Duns & Ros (1963), Aziz *et al.* (1972) or Beggs & Brill (1973) are widely employed, but in these schemes annular-mist flow is treated casually and often homogeneous flow is assumed. A more sophisticated model for wells producing gas and condensate has been proposed by Govier & Fogarasi (1975). Although derived from actual gas/condensate field data, the correlation for the liquid distribution between film and core is dimensional and thought to have little general validity. We will here investigate the accuracy with which the available data for pressure loss, film thickness and liquid entrainment can be predicted by an annular flow

model that is based on the well-known two-fluid concept. In principle, with such a model for vertical annular dispersed flow, it is possible to calculate these three physical quantities simultaneously, provided appropriate correlations are used for interfacial friction and liquid fraction entrained. Such mechanistic modelling has to be compared with that reviewed in, for example, Wallis (1969) and Hewitt & Hall-Taylor (1970). We have opted for a comparison with some recent works where complete models are offered, i.e. models including rules for both interfacial friction and liquid entrainment (Hughmark 1973; Whalley & Hewitt 1978; Hanratty & Asali 1983).

First of all, the model equations for annular dispersed flow are introduced, including the effect of entrained liquid droplets travelling with the gas in the core of the pipe (section 2). Then, using the Harwell data bank, alternative correlations are proposed for interfacial friction and liquid fraction entrained (section 3). Subsequently, the model is compared with the above-mentioned models of others (section 4). Thereafter, differences in predictions are illustrated using recent data of Azzopardi *et al.* (1983) in a 12.5 cm pipe. This is of interest because such a large diameter differs greatly from the diameters for which all the correlations were derived and therefore can act as a realistic test case for models (section 5). In section 6 implications for a hypothetical gas-well tubing of 10 cm are considered. Finally, in section 7 conclusions are drawn and suggestions for further work are made.

2. TWO-FLUID MODEL FOR ANNULAR DISPERSED FLOW

2.1. Model equations

A physical model is presented describing annular dispersed two-phase flow in vertical or near-vertical pipes. The flow pattern is illustrated in figure 1. In this pattern, the liquid is distributed over a relatively thin film at the pipe wall and entrained droplets are travelling with the gas in the core of the pipe. In the two-fluid model, the liquid at the wall is regarded as one phase and the gas plus droplets in the core as the other. The pipe has a diameter D, inclination θ and roughness ϵ. Deviation of the pipe from the vertical is allowed for by replacing the acceleration of gravity $\boldsymbol{g}$ by $\boldsymbol{g}\sin\theta$. The model is based on the following assumptions:

1. There is a steady-state, 1-D, concurrent, upward and developed two-phase flow.
2. There is no mass transfer between the gas and liquid phases.
3. The acceleration term in the momentum equations is ignored.
4. Axisymmetric flow (e.g. circumferentially uniform liquid distribution).

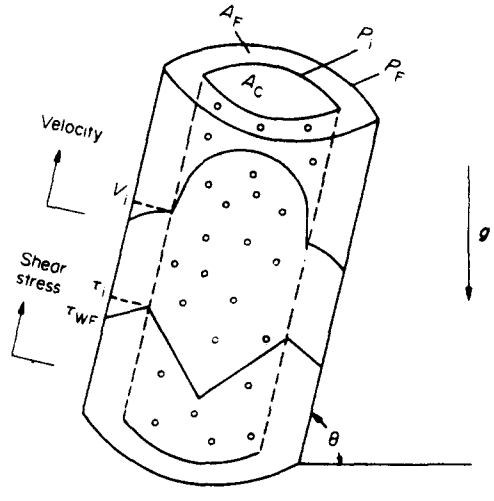

Figure 1. Annular dispersed two-phase flow.

5. The physical properties, i.e. the liquid and gas densities ρ_L and ρ_G, viscosities μ_L and μ_G and surface tension σ, are constant.
6. The liquid and gas mass flow rates W_L and W_G (or superficial liquid and gas velocities V_{SL} and V_{SG}) are given.
7. The liquid droplets in the core travel at the gas speed (homogeneous flow).

Assuming constant two-phase flow parameters is not a serious restriction, because in practice the model will be applied to a short pipe section only, and the effect of varying physical properties of the fluids along a long pipe can be evaluated by integration.

Applying momentum balances to the pipe core and the whole-pipe contents yields

$$-\frac{\partial p}{\partial z} = \rho_C \sin\theta + \frac{\tau_i P_i}{A_C} \quad [1]$$

and

$$-\frac{\partial p}{\partial z} = (\alpha_F \rho_L + \alpha_C \rho_C) g \sin\theta + \frac{\tau_{WF} P_F}{A}, \quad [2]$$

with

$$\alpha_F + \alpha_C = 1, \quad [3]$$

where

$-\frac{\partial p}{\partial z}$ = pressure loss per unit axial length,
ρ_C = core mass density,
ρ_L = liquid density,
τ_i, τ_{WF} = interfacial and wall shear stresses,
P_i, P_F = interface and wall perimeters,
$A = \pi D^2/4$ = pipe cross-section,
A_F, A_C = cross-sections occupied by film and core, respectively

and

α_F, α_C = film and core hold-ups.

The film and core hold-ups are related to the film and core cross-sections, respectively:

$$\alpha_F = \frac{A_F}{A} \quad [4]$$

and

$$\alpha_C = \frac{A_C}{A}. \quad [5]$$

The core mass density is determined from volume averaging over the core as

$$\rho_C = \frac{G_G + G_{LE}}{\frac{G_G}{\rho_G} + \frac{G_{LE}}{\rho_L}}, \quad [6]$$

where

G_G = superficial gas mass flux

$$= \frac{\text{gas mass flow rate}}{\text{total tube cross-sectional area}}$$

and

G_{LE} = superficial entrained liquid mass flux

$$= \frac{\text{entrained liquid mass flow rate}}{\text{total tube cross-sectional area}}.$$

Similarly, the core viscosity will be defined by the mixing rule as

$$\mu_C = \frac{\dfrac{G_G \mu_G}{\rho_G} + \dfrac{G_{LE} \mu_L}{\rho_L}}{\dfrac{G_G}{\rho_G} + \dfrac{G_{LE}}{\rho_L}}. \quad [7]$$

From [1] and [2] the pressure drop can be eliminated, leading to a relation from which the film hold-up α_F can be determined:

$$\frac{\tau_{WF} P_F}{A} - \frac{\tau_i P_i}{A_C} + \alpha_F \Delta\rho\, g \sin\theta = 0, \quad [8]$$

where $\Delta\rho = \rho_L - \rho_C$. The total liquid hold-up α_L follows from adding the volume fraction of liquid entrained to the film hold-up:

$$\alpha_L = \alpha_F + (1 - \alpha_F) \frac{V_{SLE}}{V_{SLE} + V_{SG}}, \quad [9]$$

where V_{SLE} is the superficial velocity of entrained liquid.

The shear stresses τ_i and τ_{WF} are calculated from

$$\tau_i = \tfrac{1}{2} f_i \left(\mathrm{Re}_C, \frac{\epsilon_i}{D_C} \right) \rho_C (V_C - V_i) |V_C - V_i| \quad [10]$$

and

$$\tau_{WF} = \tfrac{1}{2} f_F \left(\mathrm{Re}_F, \frac{\epsilon}{D} \right) \rho_L V_F^2, \quad [11]$$

where

f_i, f_F = interface and film Fanning friction factors,
V_F, V_C = average film and core velocities

and

V_i = liquid velocity at interface.

The average film and core velocities are related to the superficial film and core velocities, respectively:

$$V_F = \frac{V_{SF}}{\alpha_F} \quad [12]$$

and

$$V_C = \frac{V_{SC}}{\alpha_C}, \quad [13]$$

where the superficial velocities follow from

$$V_{SF} = \frac{G_L - G_{LE}}{\rho_L} \quad [14]$$

and

$$V_{SC} = \frac{G_G + G_{LE}}{\rho_C}. \quad [15]$$

The Fanning friction factors f_i and f_F are assumed to be functions of the corresponding pertinent Reynolds numbers

$$\mathrm{Re}_C = \frac{G_C D_C}{\mu_C} \quad [16]$$

and

$$\mathrm{Re}_F = \frac{\rho_L V_F D_F}{\mu_L}, \qquad [17]$$

and the relative interface roughness ϵ_i/D_C and relative wall roughness ϵ/D, respectively, as has been indicated in [10] and [11], where

$$G_C = (G_G + G_{LE}) = \text{core mass flux}$$

and

$$D_C, D_F = \text{core and film hydraulic diameters.}$$

The hydraulic diameters are assumed to result from

$$D_C = \frac{4A_C}{P_i} = \alpha_C^{0.5} D \qquad [18]$$

and

$$D_F = \frac{4A_F}{P_F} = \alpha_F D. \qquad [19]$$

For annular flow the film and core perimeters follow from

$$P_i = \pi(D - 2h_F) = \pi D_C \qquad [20]$$

and

$$P_F = \pi D, \qquad [21]$$

where h_F is the film thickness. The film hold-up is related to the film thickness as

$$\alpha_F = 4\frac{h_F}{D}\left(1 - \frac{h_F}{D}\right). \qquad [22]$$

For the calculation of the relative wall roughness, the pipe diameter D has been used instead of the hydraulic diameter D_F, because the latter would lead to rather unrealistic results in the limiting case of very thin films.

It should be noted that for laminar film flow a correction factor has been included in the liquid hold-up relation [8]. Employing a differential analysis of the film (velocity profile effect) modifies the gravity term by a factor $\{\alpha_F^2 - 2\alpha_C[\alpha_F + \alpha_C \ln(\alpha_C)]\}/\alpha_F^3 \simeq 0.67$; see also, Wallis (1969, p. 356), indicating that a laminar film is more easily supported against gravity than a turbulent film with the same thickness.

The above-mentioned equations form a closed set, provided relations are available for the

(1) Fanning friction factor,
(2) interface velocity V_i,
(3) interface roughness ϵ_i and
(4) liquid fraction entrained.

Unfortunately, in contrast to the foregoing mechanistic modelling, one has to rely on empirical correlations for these physical quantities. Such correlations will be discussed in section 3.

In the model the effect of droplet entrainment and deposition on the interfacial shear stress is not considered explicitly but can be considerable, as will be demonstrated subsequently. The shear stress as a result of the entrainment/deposition process is

$$\tau_d = m(V_C - V_i), \qquad [23]$$

where m is the entrainment or deposition mass flux (equilibrium assumed between these

two). The ratio of droplet shear τ_d to the friction shear τ_i can be written as

$$\frac{\tau_d}{\tau_i} = \lambda_{LE} \frac{\rho_L}{\rho_G} \frac{k}{V_{SG}^*} \frac{1}{\left(\frac{f_i}{2}\right)^{0.5}}, \quad [24]$$

assuming $\rho_C = \rho_G$, $V_C = V_{SG} \gg V_i$ and $\lambda_L \ll 1$, where k is the droplet deposition velocity and $V_{SG}^* = V_{SG}(f_i/2)^{0.5}$ is the gas friction velocity, $\lambda_L = V_{SL}/(V_{SL} + V_{SG})$ is the volume fraction of liquid and $\lambda_{LE} = (G_{LE}/G_L)\lambda_L$. Note that $m = \lambda_{LE}\rho_L k$. A maximum value for the dimensionless deposition velocity k/V_{SG}^* is about 0.2 (McCoy & Hanratty 1977; Ganic & Mastanaiah 1981; Andreussi 1983). A minimum value can be found from what is known about liquid entrainment entrance effects in annular dispersed two-phase flow. Consider a pipe section with no entrainment at the inlet and entrainment equilibrium at the outlet after a length L, where the entrainment rate equals the deposition rate. Droplet mass conservation applied to such a section, assuming a constant entrainment rate m_E and droplet deposition velocity k, gives an exponentially asymptotic approach to equilibrium with the characteristic non-dimensional length $L/D = V_{SG}/4k$. It is well-known, that entrainment equilibrium takes a larger number of diameters but is thought to happen in any case within $L/D \simeq 1000$. This maximum value for L/D leads to a minimum value for k/V_{SG}^* of about 0.004 for $f_i = 0.01$. From the above analysis, the friction-to-droplet shear ratio τ_d/τ_i would be in the range 0.6–30 for atmospheric water/air systems using $\lambda_{LE} = 0.01$. So, even the lower limit of this range indicates the effect of liquid entrainment and deposition on the interfacial shear stress to be significant. A full evaluation of the effect would require modelling of the entrainment and deposition rates, which is outside the scope of this paper. Consequently, when deriving a correlation for the interfacial shear stress further on in this paper, one cannot distinguish between the contributions from friction and droplet entrainment/deposition.

2.2. *Liquid hold-up relation*

In this section we will pay some more attention to the liquid hold-up relation [8]. For this purpose we will rewrite the hold-up relation in terms of the Lockhart–Martinelli parameter X, where

$$X^2 = \frac{f_{SL}\,\rho_L\,V_{SL}^2}{f_{SG}\,\rho_G\,V_{SG}^2}, \quad [25]$$

and the dimensionless gravity parameter

$$Y = \frac{\sin\theta}{2 f_{SG}\,\mathrm{Fr}_G^2}, \quad [26]$$

where $\mathrm{Fr}_G = (\rho_G/\Delta\rho g D)^{0.5}\,V_{SG}$ is the densimetric gas Froude number. The Fanning friction factors f_{SL} and f_{SG} are based on the corresponding Reynolds numbers and the relative wall roughness in the case that only liquid or gas would flow through the pipe. X^2 is then the ratio of the corresponding frictional pressure drops. Assuming no liquid entrainment, $V_G \gg V_i$, and a smooth pipe wall ($f_L = f_{SL}$), the hold-up relation eventually simplifies to

$$X^2 - \frac{f_i}{f_{SG}\,\alpha_G^{2.5}}\alpha_L^2 + Y\alpha_L^3 = 0, \quad [27]$$

where $\alpha_G = 1 - \alpha_L$ is the void fraction. For a given (constant) interface friction factor ratio f_i/f_{SG}, the liquid hold-up α_L only depends on the dimensionless groups X and Y, as in the Taitel & Dukler (1976) model for stratified two-phase flow. For $\alpha_L \ll 1$, and neglecting the effect of gravity ($Y = 0$), a very simple rule for the liquid hold-up is obtained:

$$\alpha_L = \left(\frac{f_{SG}}{f_i}\right)^{0.5} X. \quad [28]$$

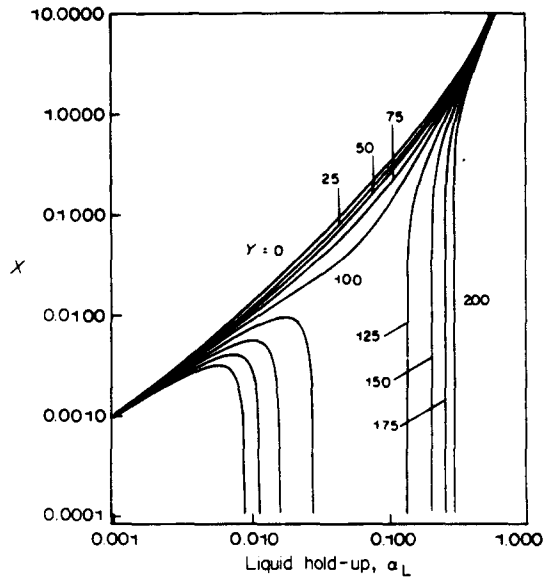

Figure 2. Lockhart–Martinelli parameter X vs liquid hold-up α_L for various values of the gravity parameter Y from the hold-up relation [27] using Wallis' interface friction factor.

However, in vertical flow the gravity term cannot be neglected generally. This has been indicated in figure 2, where the hold-up relation [27] has been plotted using the interface friction factor of Wallis (1969) for "rough" or "wavy" annular flow:

$$f_i = f_{SG}(1 + 80\,\alpha_L); \qquad [29]$$

a correlation which implies an interface (sand) roughness of about four times the film thickness; see Wallis (1969, p. 321). Note that this Wallis friction resembles what is observed in stratified two-phase flow in the sense that, at the interface, the equivalent sand roughness is about $3\sqrt{2} \simeq 4$ times the r.m.s. wave height of interface disturbances (Cohen & Hanratty 1968). This height has a maximum value of the order of that of the layer thickness. As can be seen from figure 2, the liquid hold-up is rather insensitive to gravity up till $Y \simeq 100$. However, above this value gravity has crucial effects. Gravity will cause a significant decrease of the shear stress towards the wall in the liquid film (cf. [8]). This remark refers to the annular flow models, further discussed in this paper, which model the interfacial shear stress τ_i in order to calculate the ("frictional") pressure drop. Further, gravity will lead to the occurrence of more hold-up roots, i.e. below a critical X-value and above $Y \simeq 100$, three hold-ups satisfy the hold-up relation. From a tentative investigation we concluded that it is, *a priori*, impossible to say which root has to be taken. Nor is it possible to exclude roots on account of their being physically unacceptable, e.g. from a simple stability analysis. Intuitively speaking, the middle root might seem an unstable one because a smaller liquid flow results in a larger liquid hold-up.

Depending on the flow history, in the neighbourhood of a particular root, the flow may establish at this root. Alternatively, there may be a jumping between the lowest and highest hold-up root values. At the higher root it is quite possible for liquid bridging of the pipe to occur. This idea could lead to a rule for the transition from annular to intermittent or slug flow. From figure 2, a critical Y-value of about 100 is found. For vertical flow, using $f_{SG} = 0.005$, this Y-value corresponds to $Fr_G \simeq 1$ (cf. [26]), a value close to Wallis' (1969) value of $Fr_G = 0.9$. Using the gravity group Y as a basis for the mentioned transition may have a more wider applicability than the densimetric gas Froude number Fr_G. On the other hand, for a very limited number of data points of the Harwell data bank (section 3) and for the large-diameter data of Azzopardi *et al.* (1983; section 5), apparently, annular flow is possible at the lowest of the calculated hold-up roots, assuming these data indeed belong to the annular flow regime. Consequently, an additional condition for the transition to slug flow could be that X should be larger than the local maximum in figure 2 (kind of flooding

point). Of course, this model for the transition to slug flow depends on the choice of the interface friction model and yet no definite conclusions can be drawn.

3. EMPIRICAL CORRELATIONS

3.1. Fanning friction factor

To calculate Fanning friction factors, the Colebrook (1939) equation will be employed relating the Fanning friction factor f to a Reynolds number Re and a relative roughness ϵ/D according to

$$\frac{1}{f^{0.5}} = 3.48 - 4\log\left(\frac{2\epsilon}{D} + \frac{9.35}{f^{0.5}\mathrm{Re}}\right), \quad [30]$$

for turbulent flow. For laminar flow (Re <2100),

$$f = \frac{16}{\mathrm{Re}}. \quad [31]$$

3.2. Liquid interface velocity

To obtain a value for the liquid interface velocity V_i, we propose to employ the velocity profiles known from laminar and turbulent single-phase flow. Although the model includes pipe wall roughness effects, for this velocity profile aspect a smooth pipe wall is assumed. The following universal velocity profile relation $V_i^+ = V_i^+(h_F^+)$ is used in the liquid film (Hinze 1975):

$h_F^+ \leqslant 30$ (viscous and transition or buffer layers)

$$V_i^+ = \frac{\tanh(0.074\, h_F^+)}{0.074} \quad [32]$$

$h_F^+ > 30$ (logarithmic layer)

$$V_i^+ = 2.44 \ln(h_F^+) + 4.9, \quad [33]$$

where $V_i^+ = V_i/V_F^*$ and $h_F^+ = \rho_L V_F^* h_F/\mu_L$. The wall friction velocity is

$$V_F^* = V_F\left(\frac{f}{2}\right)^{0.5}. \quad [34]$$

As the velocity profile refers to a smooth wall, the Fanning friction factor f in [34] has to be taken from a smooth wall as well.

In figure 3 the velocity ratio

$$\frac{V_i}{V_F} = V_i^+(h_F^+)\left(\frac{f}{2}\right)^{0.5} \quad [35]$$

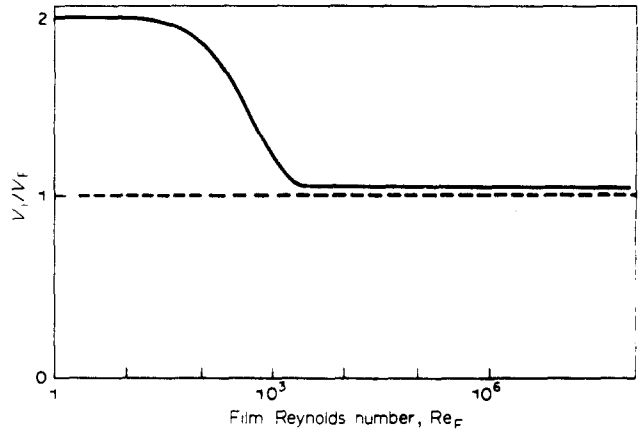

Figure 3. Relative liquid interface velocity as a function of film Reynolds number from [35].

has been plotted as a function of the film Reynolds number, illustrating this ratio to be 2 in the laminar region below $Re_F \simeq 30$, between 1 and 2 in the region between $Re_F = 30$ to 3000, and close to unity in the turbulent region. The cited procedure for the determination of the liquid interface velocity is amendable. In particular, the effect of the lifting gas core on the film velocity profile should be considered.

3.3. Interface roughness

In the two-fluid model for annular dispersed flow it has been proposed to determine the interface friction factor from an interface roughness ϵ_i and (core) Reynolds number using the Colebrook (1939) equation. A popular way to link this roughness to the interface disturbances is via

$$\epsilon_i = C\Delta h_F, \qquad [36]$$

where Δh_F is the r.m.s. wave height. If this r.m.s. wave height is larger than the average film thickness then the film thickness is used instead:

$$\epsilon_i = Ch_F. \qquad [37]$$

In this paper we will use [37] and correlate the roughness in terms of the film thickness. It is believed that too little theoretical modelling on (non-linear) finite interface wave amplitudes or experimental data on such amplitudes are available to include [36] as well. In addition to [37], it is proposed to regard the interface as smooth if the interface irregularities fall within the viscous sublayer of the core [see also Hewitt & Hall-Taylor (1970, [5, 14])], so that

$$\left.\begin{aligned} \epsilon_i &= C\left(h_F - 5\frac{\nu_G}{V_C^*}\right), \quad h_F > 5\frac{\nu_G}{V_C^*} \\ \epsilon_i &= 0, \qquad\qquad\quad h_F \leqslant 5\frac{\nu_G}{V_C^*}, \end{aligned}\right\} \qquad [38]$$

where $V_C^* = V_C(f_i/2)^{0.5}$ is the core friction velocity and ν_G is the kinematic gas viscosity.

Wallis (1969) was one of the first to offer a value for the C parameter and he proposed a value of about 4. Hughmark (1973), in his model for vertical annular flow, used an interface friction factor close to that of Wallis. Whalley & Hewitt (1978) noticed that a value of 4 was too large, in particular, for high-pressure steam/water systems. They proposed a correlation using the density ratio, viz. $C \simeq 0.3(\rho_L/\rho_G)^{0.33}$. Although this correlation greatly reduced the error in the pressure gradient predictions, the fit through the data points showed scattering of these points by more than a factor of 10. Hanratty & Asali (1983) proposed an interface friction factor based on the dimensionless film thickness h_G^+ (corresponding to the gas-phase shear velocity and kinematic viscosity) and the gas Reynolds number. As we will see in sections 4 and 6, this correlation is not satisfactory either.

In order to find an improved correlation for the interface C parameter, a data bank on vertical annular flow, compiled previously by AERE Harwell, has been employed (Whalley & Hewitt 1978). This bank contains data of various fluid systems such as water/air, ethanol/air, Genklene (trichloroethane)/air and water/steam, see table 2. The physical properties of the water/steam system come closest to those of high-pressure gas/condensate or gas/oil systems. The other fluid systems show larger differences. This has been indicated in table 1, where some important physical quantities have been compared with a gas/condensate well example. Diameters in the water/steam tests have been up to 20 mm and in the other fluid systems up to 32 mm, whereas our interest is in larger diameters, indicating a concern in diameter scaling.

The Harwell data bank contains 728 test cases for which liquid entrainment has been measured. For 527 of these tests the pressure gradient has been measured, while for 217 of these 527 tests the average film thickness is included as well. Besides the measurements by Minh & Huyghe (1965), where the L/D ratios are unknown, the L/D ratio of all other

Table 1. Comparison between fluid/pipe properties in the Harwell data bank and in a gas/condensate well example

	Harwell data bank		Gas well	
	Water/air Ethanol/air Genklene/air	Water/steam	Gas/condensate (example)	Gas/water (example)
ρ_G (kg/m^3)	<10	<56	100	100
μ_L (mPa s)	1	0.1	0.1	1
σ (N/m)	0.022–0.073	0.012–0.054	0.005	0.073
D (mm)	6–32	9–20	100	100
Re_{SL}	Laminar/turbulent	Turbulent	Turbulent	Turbulent
Fr_G	1–10	1–10	1–10	1–10

tests has been of the order of 200 or larger, considered enough to exclude entrance effects on the entrainment fraction. Table 2 contains relevant information on the test data.

C-values have been determined with our two-fluid model such that the calculated pressure losses match the measured ones (527 test cases), avoiding errors due to entrainment prediction by putting the fraction entrained equal to the fraction measured. The obtained C-values have been correlated trying various dimensionless groups (alone or in combination). In the class of one-group correlations, it appears that the Weber number,

$$We = \frac{\rho_C V_r^2 h_F}{\sigma}, \qquad [39]$$

is the most appropriate group to describe the C parameter, where $V_r = V_C - V_i$ is the relative core velocity. In figure 4 the C parameter has been plotted vs the Weber number for all test cases where the pressure gradient has been measured. Indeed, the constant value of Wallis of 4 is unsatisfactory and large differences exist with the C-values determined from our two-fluid model. A good description forms the rule

$$C = \frac{30}{We}. \qquad [40]$$

Referring to a work by Hinze (1955), this rule could be interpreted as indicating that the interface roughness is equal to the maximum diameter a liquid droplet would have in a turbulent gas stream. Although the physical significance of this remark is limited because the role of droplet entrainment/deposition on the interfacial shear stress has to be included as well, correlation wise the rule gives an improvement with respect to the others mentioned, as we will see further on in this paper. Adding the film Reynolds number as

Table 2. Test cases available in the Harwell data bank

Reference	No. of tests	Quantities measured	Fluids	D (mm)	P ($\times 10^5$ Pa)	L/D	Symbol used
Whalley *et al.* (1974)	139	*E*, *P*, *F*	A/W	31.8	2–3.5	590	□
Gill *et al.* (1964)	39	*E*, *P*, *F*	A/W	31.8	1–1.5	170	△
Gill *et al.* (1969)	9	*E*, *P*, *F*	A/W	31.8	2–3.5	520	★
Brown (1978)	30	*E*, *P*, *F*	A/W	31.8	1.7–3.1	420/560	◇
Cousins *et al.* (1965)	24	*E*, *P*	A/W	9.53	1.5–2.5	480	+
Minh & Huyghe (1965)	29	*E*, *P*	A/W	12.0	3–8	Not known	×
Minh & Huyghe (1965)	28	*E*, *P*	A/W	6.0	2–3	Not known	#
Minh & Huyghe (1965)	45	*E*, *P*	A/E	12.0	2.8–8.5	Not known	A
Cousins & Hewitt (1968a)	73	*E*, *P*	A/W	9.53	1.5–2.5	230	C
Cousins & Hewitt (1968a)	24	*E*, *P*	A/W	31.8	2	300	F
Cousins & Hewitt (1968b)	2	*E*, *P*	A/W	31.8	4	350	H
Whalley *et al.* (1974)	19	*E*, *P*	A/G	31.8	2.7	590	K
Würtz (1978)	72	*E*, *P*	S/W	10.0	30–90	900	L
Würtz (1978)	21	*E*, *P*	S/W	20.0	70	450	O
Hewitt & Pulling (1969)	72	*E*	S/W	9.3	2.4–4.5	390	T
Singh *et al.* (1969)	39	*E*	S/W	12.5	69/83	180	V
Nigmatulin *et al.* (1977)	45	*E*	S/W	13.3	10–100	300	Y
Keeys *et al.* (1970)	18	*E*	S/W	12.6	35/69	290	Z

E = liquid entrainment, P = pressure loss, F = film thickness, A = air, W = water, E = ethanol, G = Genklene, S = steam.

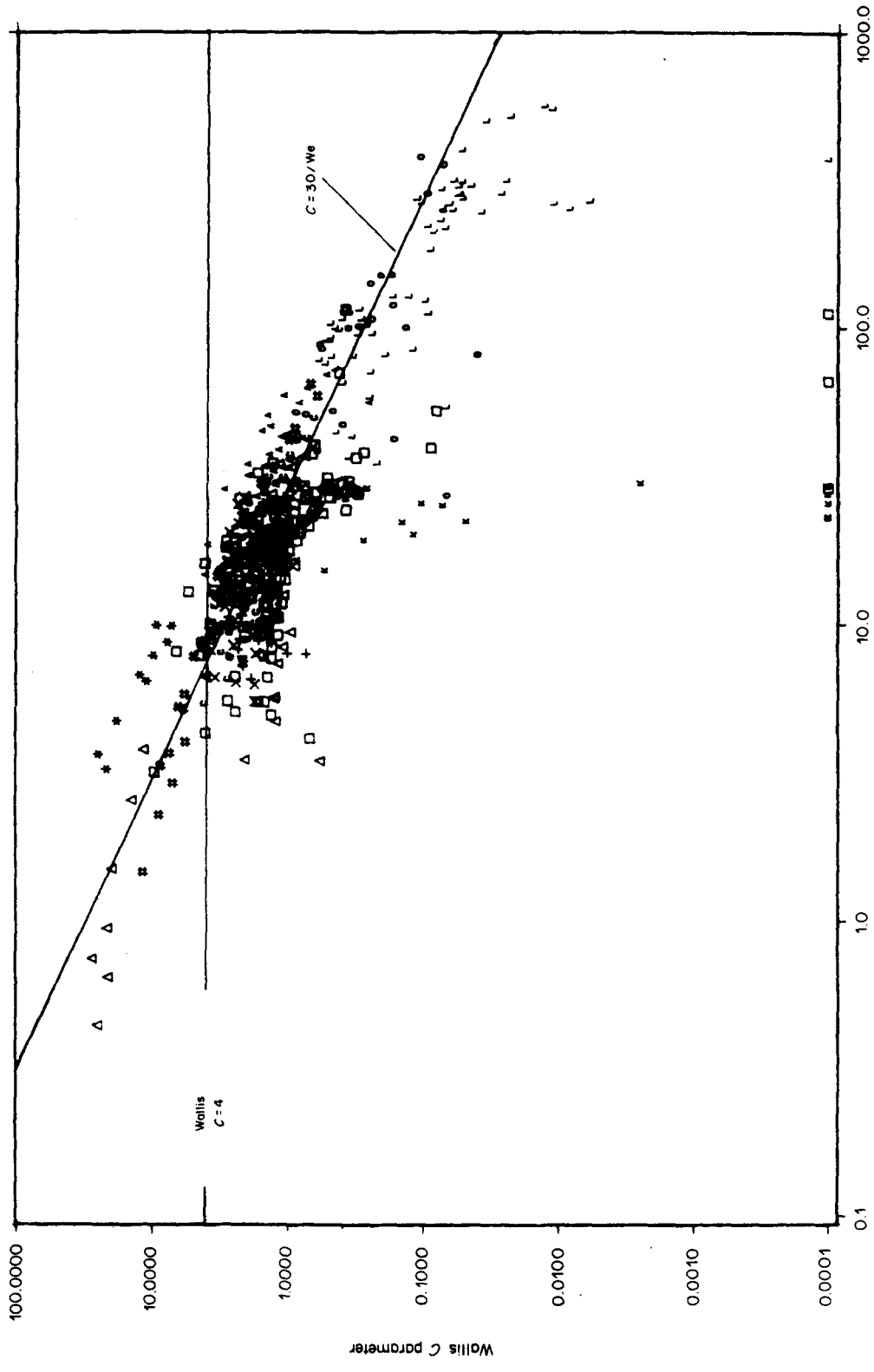

Figure 4. Wallis' C parameter vs Weber number determined from the two-fluid model using the Harwell data bank matching the calculated pressure gradient to the measured gradient. For symbols see table 2.

an extra correlating group, to take into account the state of turbulence of the film, did not improve the correlation much further and the idea was abandoned.

From all the correlation trials made, using all possible dimensionless groups, it is believed that further improvements in terms of empirical correlations, using available literature data, can hardly be achieved, probably because of inconsistencies in the test data, the tests having been carried out by different experimentalists with different facilities, fluids, diagnostics and interpretations. It is possible with new consistent and accurate measurements, carried out over large ranges of the relevant parameters, to obtain better empirical correlations, but major steps forward in the interface friction description will originate from a better physical modelling of the phenomena at the interface.

3.4. Liquid entrainment

In annular two-phase flow, the onset of liquid entrainment occurs near or above the transition from capillary waves (ripples) to large amplitude roll waves at sufficiently high gas velocities. Ishii & Grolmes (1975) developed inception criteria for droplet entrainment from simple physical models. For film Reynolds numbers $Re_F > 160$ the onset originates from the shearing-off of roll-wave crests while at lower Reynolds numbers wave undercutting was proposed. However, if the interface waves do not penetrate through the gas boundary layer, then below a minimum Reynolds number no entrainment is possible irrespective of the gas velocity. In the completely rough turbulent regime ($Re_F > 1635$), from the work by Ishii & Grolmes (1975), the critical onset gas velocity in terms of the Kutateladze number $Ku = \rho_G^{0.5}/(\Delta\rho g\sigma)^{0.25}\, V_{SG}$ varies between about 1.5 and 3. It is noted that the value of 3 is close to the Kutateladze value used by, for example, Taitel *et al.* (1980) to describe the annular to slug flow transition.

During the past 25 years a large number of empirical correlations for the fraction of liquid entrained have appeared. We mention the works by Wicks & Dukler (1960), Minh & Huyghe (1965), Paleev & Fillipovich (1966), Wallis (1968) and, more recently, Ishii & Mishima (1981). Further, correlations have been given in the annular flow models by Hughmark (1973), Whalley & Hewitt (1978) and Hanratty & Asali (1983). It should be noted that the one used by Whalley & Hewitt was originally developed by Hutchinson & Whalley (1973). After all these correlations had been compared with the measured entrainment fractions in the Harwell data bank, it was concluded that none is really satisfactory. The correlations only apply in the test range in which they were derived. Both correlation wise and from a physical point of view, the one by Hutchinson & Whalley (1973) makes most sense. Here, a dimensionless group $S = \tau_i h_F/\sigma$ is used to describe the droplet core mass concentration, where the group S gives the balance between interfacial shear and surface tension containment forces. However, it should be realized that the correlation by Hutchinson & Whalley (1973) is based on a fit through data points where the points scatter by more than a factor of 10.

Trials to improve the above-sketched situation, using the Harwell data bank, failed. No correspondence could be found with physical models such as the ones developed by Ishii & Grolmes (1975). Therefore, only empirical correlations will be considered further. The correlation model proposed is

$$\frac{E}{1-E} = 10^{\beta_0}\,\rho_L^{\beta_1}\,\rho_G^{\beta_2}\,\mu_L^{\beta_3}\,\mu_G^{\beta_4}\,\sigma^{\beta_5}\,D^{\beta_6}\,V_{SL}^{\beta_7}\,V_{SG}^{\beta_8}\,g^{\beta_9}, \qquad [41]$$

where E is the fraction of liquid entrained. A constraint is that the exponents β are chosen such that the r.h.s. of [41] forms a dimensionless group. As a result, [41] is a seven-parameter correlation (note that three dimensions are involved). In Table 3 the parameter estimates (βs) have been compiled both for the whole Harwell data bank and for subgroups after dividing the bank into a number of intervals based on the film Reynolds number. The parameter estimates for the whole bank show liquid entrainment to increase most significantly with pipe diameter and superficial gas velocity and to decrease with surface tension. The standard error of the estimates is small but misleading, as can be demonstrated by examining the parameter estimates for the subgroups. Some parameters

Table 3. Parameter estimates for the entrainment correlation model [43] from the Harwell data bank

Parameter	Corresponding physical quantity	All data points		Parameter estimates film Reynolds number intervals					
		Parameter estimate	Standard error	100–300	300–10^3	10^3–3×10^3	3×10^3–10^4	10^4–3×10^4	3×10^4–10^5
β_0	Intercept	−2.52	0.40	−0.69	−1.73	−3.31	−8.27	−6.38	−0.12
β_1	ρ_L	1.08	0.05	0.63	0.94	1.15	0.77	0.89	0.45
β_2	ρ_G	0.18	0.06	0.96	0.62	0.40	0.71	0.70	0.25
β_3	μ_L	0.27	0.04	−0.80	−0.63	−1.02	−0.13	−0.17	0.86
β_4	μ_G	0.28	0.11	0.09	0.50	0.46	−1.18	−0.55	−0.05
β_5	σ	−1.80	0.08	−0.88	−1.42	−1.00	−0.17	−0.87	−1.51
β_6	D	1.72	0.05	2.45	2.04	1.97	1.16	1.67	0.91
β_7	V_{SL}	0.70	0.03	0.91	1.05	0.95	0.83	1.04	1.08
β_8	V_{SG}	1.44	0.05	−0.16	0.96	0.78	1.45	1.27	0.71
β_9	g	0.46	0.03	0.86	0.48	0.41	−0.32	0.07	0.21
No. of points		727		40	206	224	76	102	74

show a clear tendency while other ones show a more whimsical behaviour with the film Reynolds number. For instance, the diameter parameter (β_6) is a decreasing function with Re_F, i.e. the effect of the diameter on liquid entrainment is stronger at laminar flow than at turbulent film flow. We will not attach any interpretation to these findings because an underlying physical model is lacking. The above correlation model and subdivision are casual. Other models and subdivisions were tested but they gave results of similar nature and similar or lower quality.

Although some of the physical quantities show little, none or a correlated variation in the bank, leading to possibly unreliable parameter estimates, the whimsical behaviour of parameter estimates in the correlation models may point to inconsistencies in the data bank. As entrance effects, the gas expansion effect and the measurement of the entrained fraction all need close attention in liquid entrainment studies, such inconsistencies are not unlikely.

Too few data at very low film Reynolds numbers ($Re_F < 100$) are available in the bank. Therefore, a correlation for a minimum Reynolds number below which no entrainment is possible, could not be developed. In order to allow for a minimum film fraction, it is suggested to use some rule based on the penetration of interface waves through the gas boundary layer, like the one proposed by Ishii & Grolmes (1975):

$$(Re_F)_{min} = \left[\frac{y^+}{0.347}\left(\frac{\rho_L}{\rho_G}\right)^{1/2}\frac{\mu_G}{\mu_L}\right]^{3/2}; \qquad [42]$$

Ishii & Grolmes used $y^+ = 10$.

4. COMPARISON WITH OTHER MODELS

Using the Harwell data bank, we will compare our two-fluid-model (also referred to as the KSLA model) with those of Hughmark (1973), Whalley & Hewitt (1978) and Hanratty & Asali (1983). These authors have been chosen because they offer complete annular flow models, including rules for the film thickness, liquid entrainment and interface friction. The models will be described briefly below, without details.

In the model of Hughmark (1973), the film thickness is determined from an empirical correlation between the dimensionless film thickness h_F^+ and the film Reynolds number Re_F. For the liquid entrainment a correlation was developed based on the dimensionless film thickness h_G^+, which is related to h_F^+ as defined above: $h_G^+ = (\rho_G/\rho_L)^{0.5}(\mu_L/\mu_G)h_F^+$. The pressure drop is linked to an interface friction factor close to that of Wallis (1969). Hughmark's correlations are based on a limited number of tests showing little parameter variation. He claims his model to be valid for a maximum tube diameter of about 4 cm and a maximum liquid viscosity of about 5 mPa s.

In the model of Whalley & Hewitt (1978), a form of the triangular relation is used to determine the film thickness. The film friction factor needed in this relation is the one plotted against film Reynolds number by Hewitt & Hall-Taylor (1970) from numerical data by Hewitt (1961). The model features the earlier-mentioned Hutchinson & Whalley (1973) entrainment correlation. In their interface friction factor, compared to the one by Wallis (1969), the density has been introduced as has been explained in the preceding section. The data used for the correlations of Whalley & Hewitt are the same as those employed in our study.

In the model of Hanratty & Asali (1983), the film thickness is determined from the same type of correlation as that of Hughmark. Liquid entrainment has been correlated from a dimensional group $\rho_L^{0.5}\rho_G^{0.5}V_G^3 D^{2.25}$. Maximum possible entrainment follows from a critical film Reynolds number based on the transition to roll waves. It is noted that in the models of Hughmark and Whalley & Hewitt entrainment is automatically limited because the entrainment depends on the film thickness. Although Hanratty & Asali do not give a quantitative rule for the effect of surface tension, on the basis of their figures, we included this effect in their entrainment correlation. Their interface friction factor has been mentioned in the preceding section. Hanratty & Asali employ data also present as part

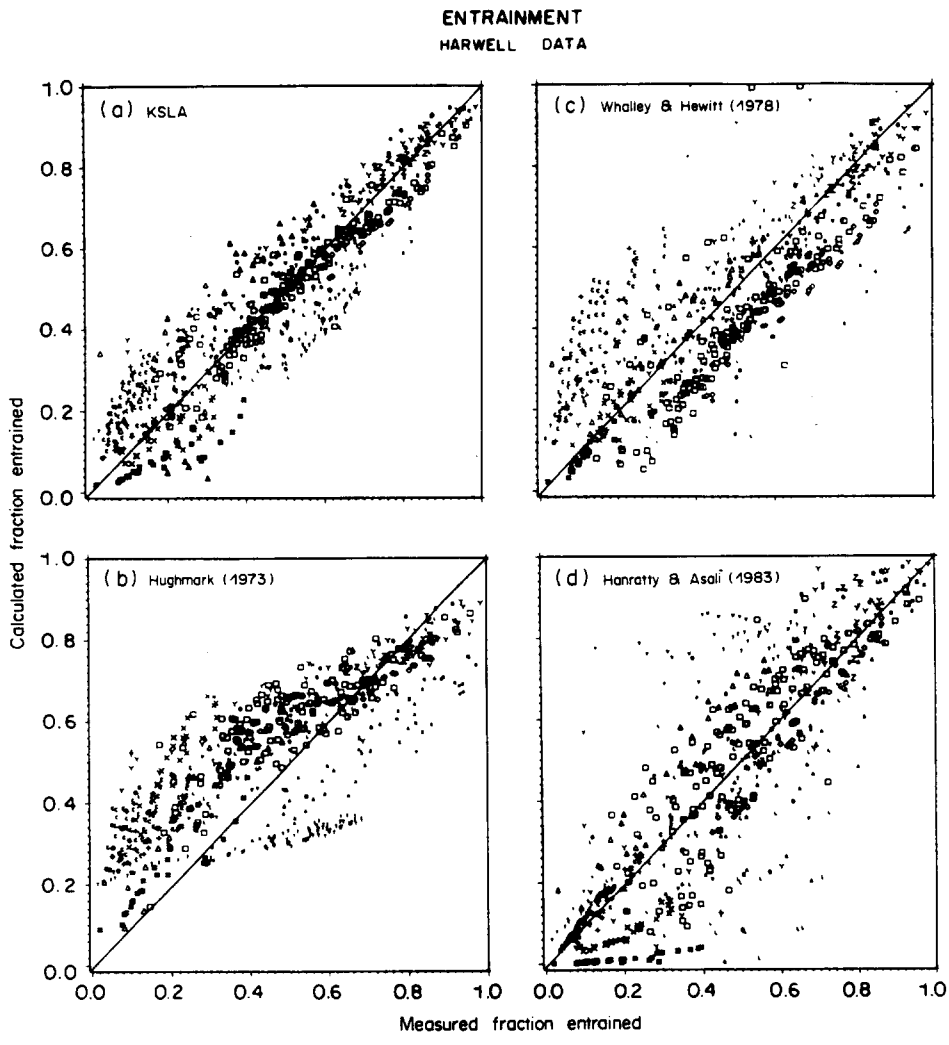

Figure 5. Calculated fraction of liquid entrained vs measured fraction for the two-fluid model and the three literature models employing the Harwell data bank. For symbols see table 2.

of the Harwell data bank. Additionally, data from 2.29 and 4.2 cm pipes, in which the liquid viscosity was varied from 1.1 to 4.6 mPa s, have been used.

In the three models just described, homogeneous flow is assumed in the core. Gravity effects, which will play a role at the lower side of the annular flow regime, are not included. To take the hydrostatic head effect correctly into account in these models, we added the core head to the calculated pressure drop (cf. [1]). The models have been solved numerically using a generalized Newton–Raphson technique.

Figures 5a–d show the calculated fraction of liquid entrained vs the measured fraction for all Harwell data points using our two-fluid model and the three literature models. Even with the best fit of the Harwell data bank, which we use, there remains a large scatter of the data points (cf. figure 5a). Furthermore, systematic discrepancies exist between calculated and measured data, pointing to inconsistencies in the bank and/or the impossibility to describe liquid entrainment with simple empirical correlation models.

Evidently, Hughmark's entrainment correlation (Figure 5b) follows a different trend with the dimensionless film thickness h_G^+, than the Harwell experimental data. Furthermore, some systems [e.g. tests by Hewitt & Pulling (1969)] show a trend completely different from the bulk of the data. Surprisingly, although surface tension was not considered, high-pressure water/steam data (σ down to 0.012 N/m) fall in this bulk. Also the entrainment correlation used by Whalley & Hewitt (1978) (figure 5c) shows large scatter and systematic discrepancies between calculated and measured data [e.g. tests by

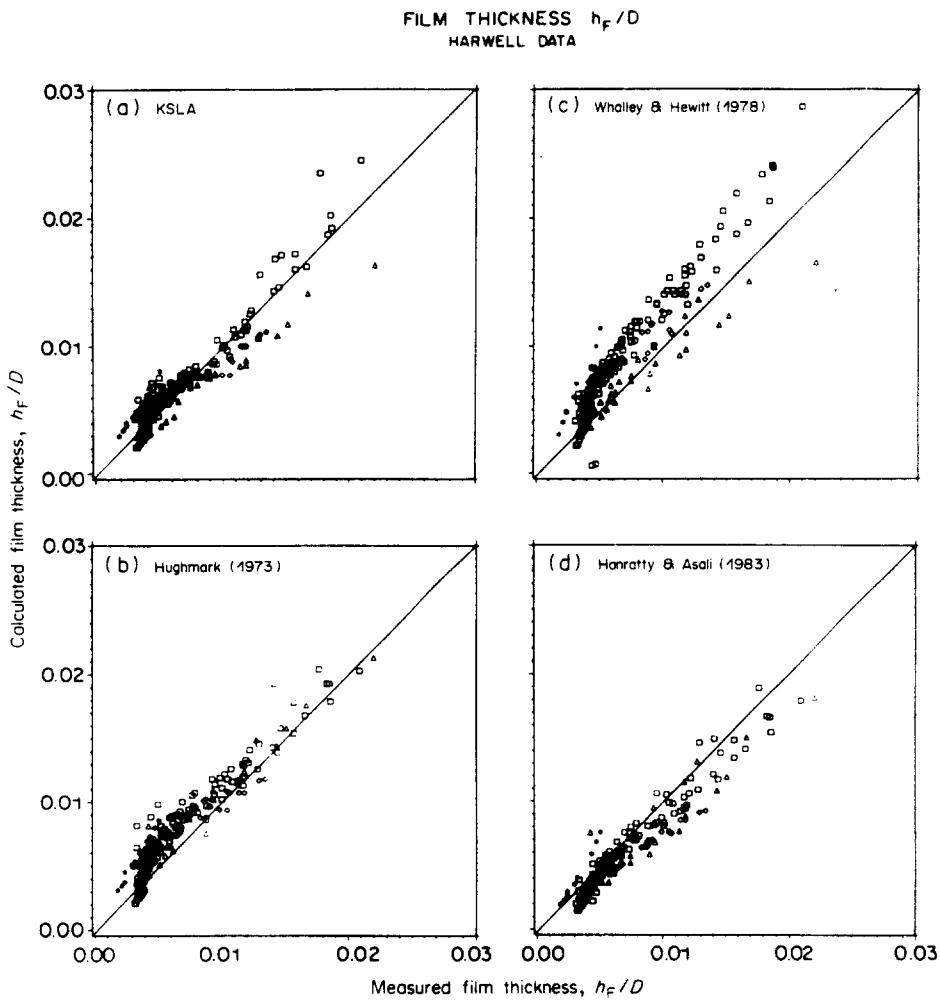

Figure 6. Calculated relative film thickness vs measured thickness for the two-fluid model and the three literature models employing the Harwell data bank. For symbols see table 2.

Cousins & Hewitt (1968a)]. Finally, the correlation by Hanratty & Asali (1983) gives points in figure 5d more or less all over the place. In sum, none of the empirical entrainment correlations is able to describe liquid entrainment correctly, even when applied to the same, or same type of, data from which these correlations were derived. This puts considerable doubt on their predictive value.

Figures 6 a–d show the calculated relative film thickness (h_F/D) vs the measured one (217 data points). Even though film thickness is strongly interrelated to entrainment, which latter quantity has a low accuracy, the film thickness is reproduced with good accuracy. The film thickness by Whalley & Hewitt is somewhat overpredicted, whereas the other models show comparable reproduction of the data. The bulk of the points fall here within $\pm 20\%$ accuracy limits. Unfortunately, film thickness information is limited to low-pressure water/air systems in the Harwell data bank so that no comparison can be made for other fluid systems and high pressures.

Finally, figures 7a–d show the calculated pressure gradient vs the measured gradient (527 data points). The pressure gradient is strongly linked to the interface friction. Figure 7a demonstrates that our interface C parameter in terms of the Weber number leads to a reasonably accurate pressure-drop reproduction. The one by Whalley & Hewitt gives slightly more scatter. Hughmark's (1973) interface friction leads to an overestimation of pressure losses by up to a factor of about 3 for the high-pressure water/steam data of Würtz (1978). The pressure-drop predictions by Hanratty & Asali can also be too large by a factor of more than 2.

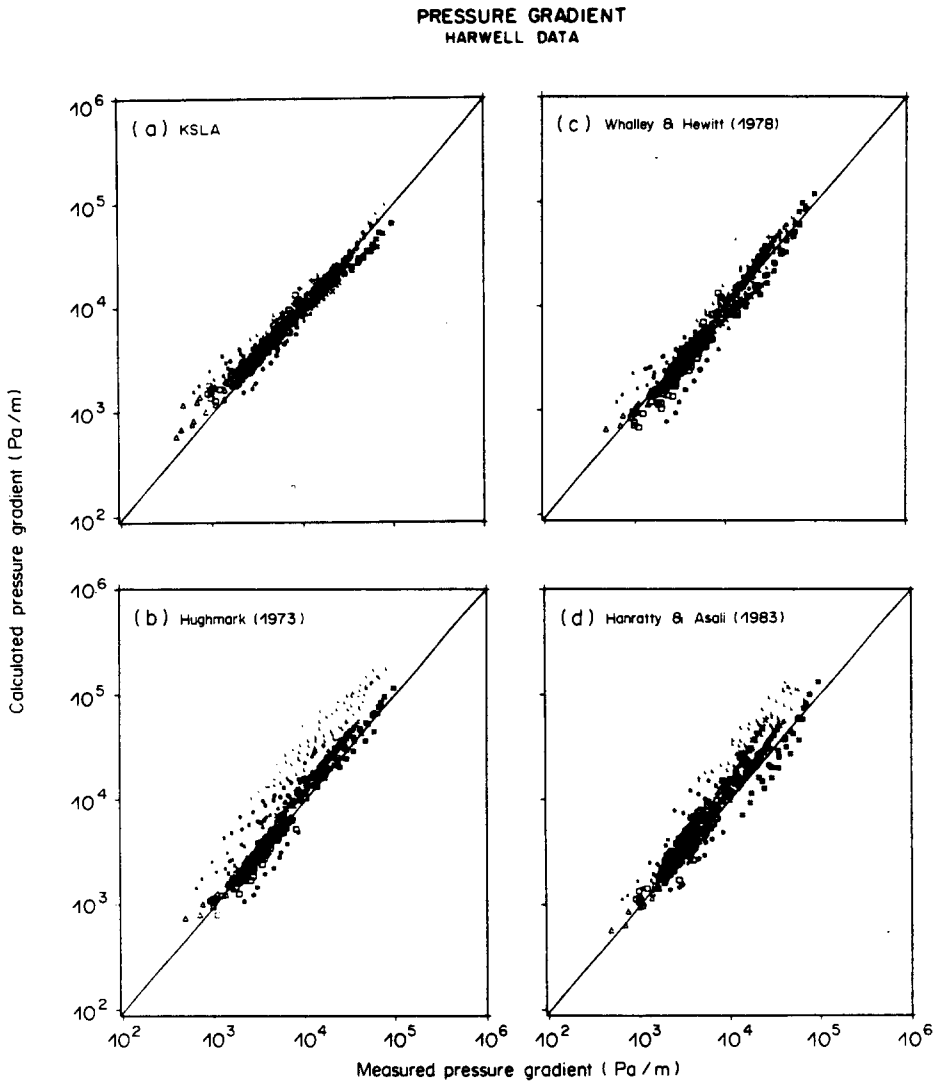

Figure 7. Calculated pressure gradient vs measured gradient for the two-fluid model and the three literature models employing the Harwell data bank. For symbols see table 2.

5. TESTING OF MODELS WITH 12.5 cm PIPE DATA

Large-diameter test data on annular two-phase flow have been reported by Azzopardi *et al.* (1983). Experiments were carried out in a vertical 12.5 cm pipe using water/air at atmospheric conditions. Large-diameter test data are not available in the Harwell data bank and therefore the data of Azzopardi *et al.* can serve to test the annular flow models outside the range in which the empirical correlations, needed in these models, were derived.

Figure 8 shows measured liquid fractions entrained compared to those from our best fit of the Harwell data bank (subsection 3.4) and the three literature models (section 4). In this figure data are plotted as a function of the gas mass flux for a fixed liquid mass flux of 2.6 kg/m^2 s. The best fit of the Harwell data bank strongly overpredicts the entrainment. The Whalley & Hewitt (1978) model shows a wrong trend. Apparently, the models of Hughmark (1973) and Hanratty & Asali (1983) give the best estimates, but as these latter two models gave rather unreliable estimates when the Harwell data bank was employed (see preceding section), it is believed that the agreement is more of a coincidental nature. Figure 9 is a plot similar to figure 8, but with a higher liquid mass flux of 10.3 kg/m^2 s. Again, the Whalley & Hewitt model shows a wrong trend, while the other three models overpredict entrainment by some 40%. In short, comparing present

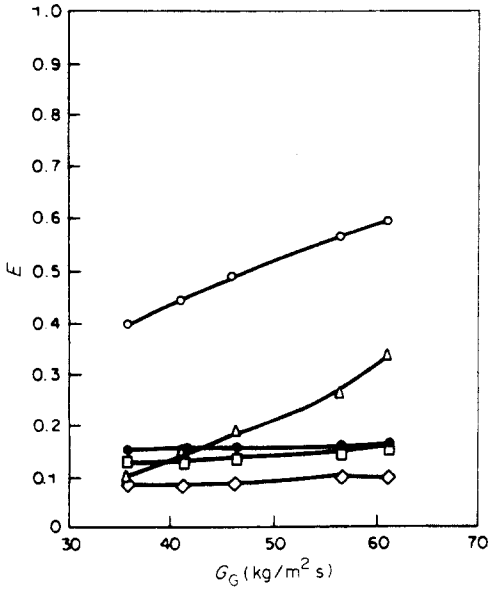

Figure 8. Experimental large-diameter entrainment data compared to estimates from the best fit of the Harwell data bank and the three literature models. 12.5 cm pipe, atmospheric air/water (Azzopardi *et al.* 1983). ◇, Tests $G_L = 2.6$ kg/m² s; ○, best fit Harwell data bank; □, Hughmark (1973); △, Whalley & Hewitt (1978); ●, Hanratty & Asali (1983).

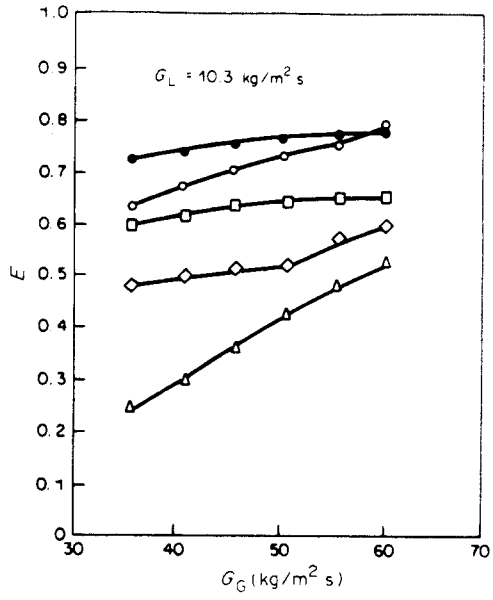

Figure 9. As for figure 8 but higher liquid mass flux.

entrainment correlations with large diameter test data does not give much further confidence in the predictive value of these correlations.

Figure 10 shows measured pressure gradients compared to those from the KSLA and Whalley & Hewitt models as a function of the liquid mass flux for a fixed gas mass flux of 35.9 kg/m² s. The Whalley & Hewitt model underpredicts the pressure losses by more than a factor of 2. Examining in more detail the output of the Whalley & Hewitt model, it appears that there is a physical conflict due to the omission of gravity. Gravity begins to play a role in larger diameter pipes (see gravity parameter, [26]). Taking as an example mass fluxes $G_L = 41.2$ kg/m² s and $G_G = 35.9$ kg/m² s, leads to a film hold-up of about 2.5%. The hydrostatic head corresponding to this hold-up is of the order of the calculated

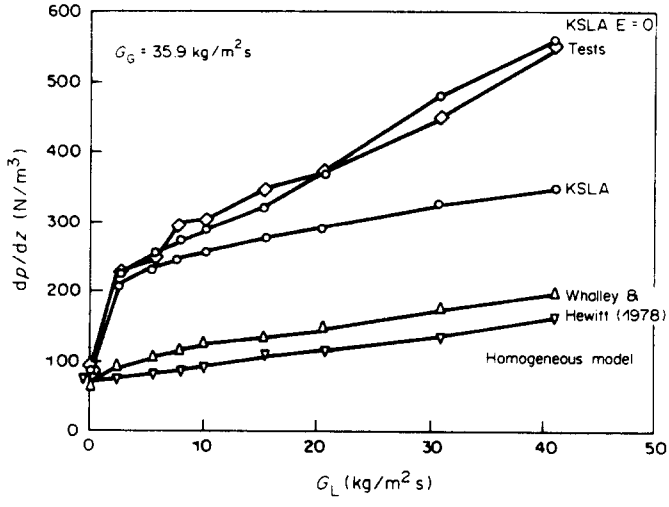

Figure 10. Experimental large-diameter pressure gradients compared to various annular flow models. Details/symbols as in figure 8.

pressure drop from the interfacial shear stress. Consequently, it is necessary to account for gravity more correctly and to take into account the decrease of the shear stress in the film towards the wall (cf. [8]). The models of Hughmark and Hanratty & Asali give similar results to the Whalley & Hewitt model and have therefore not been plotted in Fig. 10. The KSLA model gives an improvement in pressure loss prediction, but still losses are underpredicted. Setting, on purpose, the entrainment equal to zero in the KSLA model results in pressure gradients almost identical with the measured ones, indicating the effect of entrainment on the pressure drop. However, it does not explain the disagreement observed because, in particular, at the higher liquid mass fluxes, the discrepancy between the calculated and measured fractions entrained is small. The pressure gradients of the homogeneous model are shown in figure 10. Evidently, this approach cannot be used.

6. IMPLICATIONS FOR GAS WELLS

Implications for two hypothetical high-pressure gas-well examples will be considered. In the first example a gas/condensate system is studied in a tube of 10 cm dia. The condensate density is 500 kg/m^3, the condensate viscosity is 0.1 mPa s and the surface tension is 0.005 N/m. In the second example the condensate is replaced by water having a density of 1000 kg/m^3, a liquid viscosity of 1 mPa s and a surface tension of 0.073 N/m. In both examples the gas density is 100 kg/m^3 and the gas viscosity is 0.02 mPa s. Further, the liquid volume fraction is 2%.

Figure 11 shows the liquid fraction entrained as a function of the superficial gas velocity for the two above-mentioned examples. At the lowest gas velocities shown, the densimetric gas Froude number is about 1, corresponding to the lower side of the annular flow regime. At this lower side, for the condensate example, entrainment predictions by the various models differ appreciably (50–98%). Above a gas velocity of 10 m/s all models predict entrainment to be >95%. At $V_{SG} = 20$ m/s, entrainment in the KSLA and Hanratty & Asali (1983) models is >99.9%, leaving only a very thin, laminar film at the pipe wall ($h_F/D < 0.0001$, $Re_F < 100$). In the Hughmark (1973) and Whalley & Hewitt (1978) models entrainment is more limited, leaving a thicker film ($h_F/D = 0.0008$ and $h_F/D = 0.0005$, respectively) in the transition/turbulent mode. Of course, the water example shows less entrainment due to the higher surface tension, except for Hughmark's model in which surface tension is not considered. At $V_{SG} = 10$ m/s entrainment predictions vary from about 50 to 98%. Film thickness predictions appear to vary here by a factor of about 10.

Figure 12 shows the pressure gradient for the two gas-well examples. Difference between the various models stay within a factor of 2 for the condensate example. However, for the

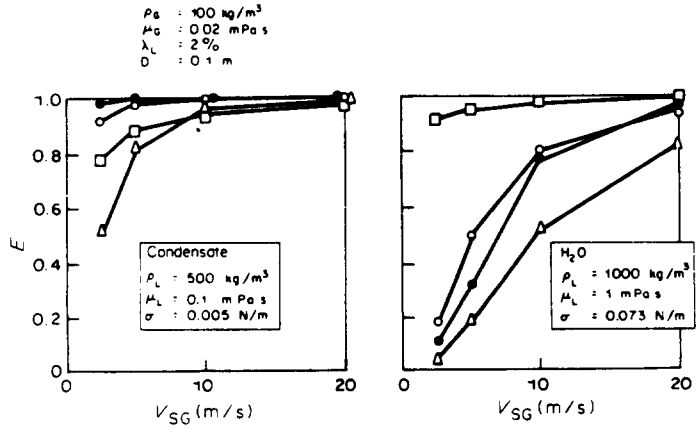

Figure 11. Liquid fraction entrained as a function of superficial gas velocity; calculations from various annular flow models: ○, KSLA; □, Hughmark (1973); △, Whalley & Hewitt (1978); ●, Hanratty & Asali (1983).

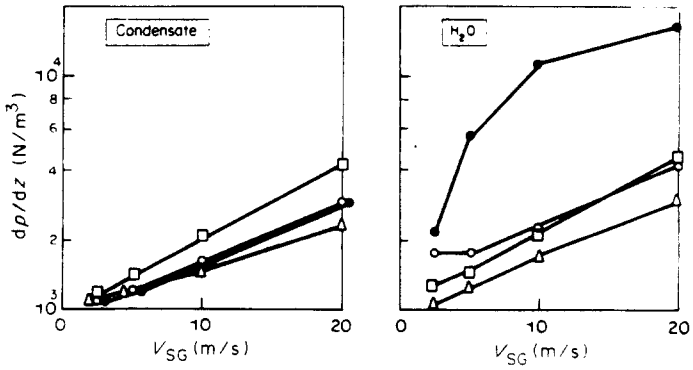

Figure 12. Pressure gradient as a function of superficial gas velocity; calculations from various annular flow models, as given in figure 11.

water example the model of Hanratty & Asali gives predictions completely different from those of the other models. It is noted that the homogeneous model gives pressure gradients close to those of Hughmark's model.

7. CONCLUSIONS

The two-fluid concept can conveniently be used to describe annular dispersed flow, since it accounts for the interrelation between pressure loss, film thickness and liquid fraction entrained. The liquid hold-up relation resulting from such a concept may give rise to several hold-up roots due to the effect of gravity, in particular for large-diameter tubes. In situations where gravity effects cannot be ignored the approach of the "simple triangular relationship" is not allowed. Pressure-drop predictions can be improved with respect to existing annular flow models by correlating the interface friction in terms of the Weber number, as suggested by the data in the Harwell data bank. Unfortunately, it is not possible to distinguish between the contributions from actual gas friction and friction from droplet deposition/entrainment. Efforts to improve the empirical description of liquid entrainment failed and demonstrated inconsistencies in literature test data and/or the impossibility to describe entrainment with simple empirical correlation models. Application of existing entrainment correlations gives rise to widely varying results and the predictive value of these correlations is rather low. Extrapolation of present methods for annular flow to large-pipe and/or high-pressure systems is hazardous. Nevertheless, it is believed that the most realistic results are obtained using the model presented in this paper or the model of Whalley & Hewitt (1978).

To improve the predictive ability of the models, further work is needed. In the first place, consistent test data from experiments carried out over large ranges of the relevant parameters are still needed in order to derive better rules for interface friction and liquid entrainment. For the oil industry, vertical annular flow tests should be carried out in large-diameter pipes (100–150 mm) at high pressure (5–10 MPa). Although in this industry often field data are available on pressure drop (e.g. gas wells), allowing some verification of a model, further characteristics such as film thickness or liquid entrainment are much more difficult to obtain; hence such data are unsuitable for a real development of models. In the second place, mechanistic models should be developed for the droplet entrainment/deposition process which can be implemented in two-fluid models for determining both the fraction of liquid entrained and the contribution of this process to the interface friction.

REFERENCES

ANDREUSSI, P. 1983 Droplet transfer in two-phase annular flow. *Int. J. Multiphase Flow* **9**, 697–713.

AZIZ, K., GOVIER, G. W. & FOGARASI, M. 1972 Pressure drop in wells producing oil and gas. *J. Can. Petrol. Technol.* **11**, 38–44.

AZZOPARDI, B. J., TAYLOR, S. & GIBBONS, D. B. 1983 Annular two-phase flow in a large diameter tube. *Int. Conf. on the Modelling of Multiphase Flow*, Coventry, W. Midlands, 19–21 April, Paper F4.

BEGGS, H. D. & BRILL, J. P. 1973 A study of two-phase flow in inclined pipes. *J. Petrol. Technol.* **May**, 607–617.

BROWN, D. J. 1978 Disequilibrium annular flow. Ph.D. Thesis, Univ. of Oxford, Oxon.

BROWN, D. J., JENSEN, A. & WHALLEY, P. B. 1975 Non-equilibrium effects in heated and unheated annular two-phase flow. ASME Paper No. 75-WA/HT-7.

COHEN, L. S. & HANRATTY, T. J. 1968 Effects of waves at a gas/liquid interface on turbulent air flow. *J. Fluid Mech.* **31**, 467–479.

COLEBROOK, C. F. 1939 Turbulent flow in pipes with particular reference to the transition region between the smooth and rough pipe laws. *J. Instn civ. Engrs* **11**, 133.

COUSINS, L. B. & HEWITT, G. F. 1968a Liquid phase mass transfer in annular two-phase flow: droplet deposition and liquid entrainment. Report AERE-R 5657, UKAEA, Harwell, Oxon.

COUSINS, L. B. & HEWITT, G. F. 1968b Liquid phase mass transfer in annular two-phase flow: radial liquid mixing. Report AERE-R 5693, UKAEA, Harwell, Oxon.

COUSINS, L. B., DENTON, W. H. & HEWITT, G. F. 1965 Liquid mass transfer in annular two-phase flow. *Two-phase Flow Symp.*, Exeter, Devon, Paper C4.

DUNS, H. & ROS, N. C. J. 1963 Vertical flow of gas and liquid mixtures in wells. *Proc. 6th Wld Petroleum Congr.*, Frankfurt, Paper 22, pp. 451–465.

GANIC, E. N. & MASTANAIAH, K. 1981 Investigation of droplet deposition from a turbulent gas stream. *Int. J. Multiphase Flow* **7**, 401–422.

GILL, L. E., HEWITT G. F. & LACEY, P. M. C. 1964 Sampling probe studies of the gas core in annular two-phase flow. Part 2. Studies of the effect of phase flow rates on phase and velocity distribution. *Chem. Engng Sci.* **19**, 665–682.

GILL, L. E., HEWITT, G. F. & ROBERTS, D. N. 1969 Study of the behaviour of disturbance waves in annular flow in a long vertical tube. Report AERE-R 6012, UKAEA, Harwell, Oxon.

GOVIER, G. W. & FOGARASI, M. 1975 Pressure drop in wells producing gas and condensate. *J. Can. Petrol. Technol.* **14**, 28–42.

HANRATTY, T. J. & ASALI, J. C. 1983 Entrainment measurement and their use in design equations. *Report to Members of the Design Institute for Multiphase Processing*, Nov.

HEWITT, G. F. 1961 Analysis of annular two-phase flow: application of the Dukler analysis to vertical upward flow in a tube. Report AERE-R 3680, UKAEA, Harwell, Oxon.

HEWITT, G. F. & HALL-TAYLOR, N. S. 1970 *Annular Two-phase Flow*. Pergamon Press, Oxford.

HEWITT, G. F. & PULLING, D. J. 1969 Liquid entrainment in adiabatic steam–water flow. Report AERE-R 5374, UKAEA, Harwell, Oxon.

HINZE, J. O. 1955 Fundamentals of the hydrodynamic mechanism of splitting in dispersion process. *AIChE Jl* **1**, 289–295.

HINZE, J. O. 1975 *Turbulence*, 2nd edn. McGraw-Hill, New York.

HUGHMARK, G. A. 1973 Film thickness, entrainment and pressure drop in upward annular and dispersed flow. *AIChE Jl* **19**, 1062–1065.

HUTCHINSON, P. & WHALLEY, P. B. 1973 A possible characterization of entrainment in annular flow. *Chem. Engng Sci.* **28**, 974–975.

ISHII, M. & GROLMES, M. A. 1975 Inception criteria for droplet entrainment in two-phase concurrent film flow. *AIChE Jl* **21**, 308–318.

ISHII, M. & MISHIMA, K. 1981 Correlation for liquid entrainment in annular two-phase flow of low viscous fluid. Report ANL/RAS/LWR/81-2, ANL, Argonne, Ill.

KEEYS, R. K. F., RALPH, J. C. & ROBERTS, D. N. 1970 Liquid entrainment in adiabatic steam-water flow at 500 and 1000 psia. Report AERE-R 6293, UKAEA, Harwell, Oxon.

McCoy, D. D. & Hanratty, T. J. 1977 Rate of deposition of droplets in annular two-phase flow. *Int. J. Multiphase Flow* **3**, 319–331.

Minh, T. Q. & Huyghe, J. D. 1965 Some hydrodynamical aspects of annular dispersed flow, entrainment and film thickness. *Two-phase Flow Symp.*, Exeter, Devon, Paper C2. (See also Minh, T. Q. Contribution to the study of annular two-phase flow. Ph.D. Thesis, Univ. of Grenoble, Grenoble, France.)

Nigmatulin, B. I., Malyshenko, V. I. & Shugaev, Y. Z. 1977 Investigation of liquid distribution between the core and the film in annular dispersed flow of steam/water mixtures. *Therm. Engng* **23**, (5), 66–68.

Paleev, I. I. & Fillipovich, B. S. 1966 Phenomena of liquid transfer in two-phase dispersed annular flow. *Int. J. Heat Mass Transfer* **9**, 1089–1093.

Singh, K., St Pierre, C. C., Crago, W. A. & Moeck, E. O. 1969 Liquid film flow rates in two-phase flow of steam and water at 1000 psia. *AIChE Jl* **15**, 51–56. (See also Singh, K. 1967 Liquid film flow-rate measurements at elevated pressures. M.Sc. Thesis, Univ. of Windsor, Windsor, Ontario.)

Taitel, Y. & Dukler, A. E., 1976 Modelling flow pattern transitions in horizontal and near-horizontal gas–liquid flow. *AIChE Jl* **22**, 47–55.

Taitel, Y., Barnea, D. & Dukler, A. E. 1980 A model for predicting flow regime transition for steady upward gas–liquid flow in vertical tubes. *AIChE Jl* **26**, 345–354.

Wallis, G. B. 1968 Phenomena of liquid transfer in two-phase dispersed annular flow. *Int. J. Heat Mass Transfer* **11**, 783–785.

Wallis, G. B. 1969 *One-dimensional Two-phase Flow*. McGraw-Hill, New York.

Whalley, P. B. & Hewitt, G. F. 1978 The correlation of liquid entrainment fraction and entrainment rate in annular two-phase flow. Report AERE-R 9187, UKAEA, Harwell, Oxon.

Whalley, P. B., Hewitt, G. F. & Hutchinson, P. 1974 Experimental wave and entrainment measurements in vertical annular two-phase flow. *Symp. on Multi-phase Flow Systems*, Univ. of Strathclyde, Strathclyde, Scotland, Paper A1.

Wicks, M. & Dukler, A. E. 1960 Entrainment and pressure drop in concurrent gas–liquid flow: air–water in horizontal flow. *AIChE Jl* **6**, 463–468.

Würtz, J. 1978 Entrainment in annular steam-water flow. *Eur. Two-phase Flow Gp Mtg*, Stockholm, Sweden.